Available online at www.sciencedirect.com
SCIENCE DIRECT®
Journal of Power Sources 118 (2003) 325–333
JOURNAL OF POWER SOURCES
www.elsevier.com/locate/jpowsour

Characterization of Pt-based catalyst materials by voltammetric techniques

U. Koponen[a,*], H. Kumpulainen[b], M. Bergelin[a], J. Keskinen[b], T. Peltonen[b], M. Valkiainen[b], M. Wasberg[c]

[a]*Åbo Akademi, Process Chemistry Group, c/o Combustion and Materials Chemistry, Biskopsgatan 8, FIN-20500 Åbo, Finland*
[b]*VTT Technical Research Centre of Finland, VTT Processes, P.O. Box 1601, FIN-02044 VTT, Finland*
[c]*Kemira Chemicals Oy, Oulu Research Centre, P.O. Box 171, FIN-90101 Oulu, Finland*

Abstract

Catalyst materials in form of inks, as half-MEAs and inside a polymer electrolyte membrane unit cell were characterized by cyclic voltammetry. Laboratory made Pt inks were modified with Ru, Os and Ru + Ir and the methanol oxidation activity of the created surfaces was tested. A novel electrode, which enables the study of the oxygen reduction reaction on the cathode was introduced. With the measuring device it was possible to vary the oxygen content on the ink side and the proton activity of the electrolyte on the membrane side of a half-MEA. Catalyst layers based on Pt, Pt-Ru and Pt-Co inside a PEM-unit cell were also characterized in situ by cyclic voltammetry. The active surface areas were found to be linearly dependent on the Pt mass density in the catalyst layers. Approximately 30% of the Pt loading in the MEAs were electroactive.

Keywords: Pt; Voltammetry; Fuel cell catalyst; Methanol

1. Introduction

Cyclic voltammetry is a commonly used technique for the study of surface processes and has been used in several investigations on catalyst materials based on Pt. Cyclic voltammetry enables, for example, comparison of electrocatalytic properties of Pt catalysts manufactured or pre-treated in different ways. In low temperature polymer electrolyte membrane fuel cells (PEMFC) nano-sized Pt particles supported on high surface area carbon is the most frequently used electrocatalyst on both the anode and the cathode side. Cyclic voltammetry also provides the ability to determine the active surface area of Pt catalysts. Several studies on this subject have been made for Pt nanoparticles on different supports. Pt/C water suspensions [1] and Pt inks [2,3] have been deposited onto glassy carbon (GC) electrodes. GC has also been used as the support for vacuum evaporated Pt. [4–6]. In other studies, Au has been used as the support material for colloidal Pt and Pt/C suspensions [7,8] as well as for Pt hydrosols [9]. In one study [10], Pt particles were directly formed by electrochemical reduction onto a Nafion 117 membrane whereas in another study [11], Pt was both electrolessly and electrochemically applied onto highly oriented pyrolytic graphite. In a recent study [12] again, Pt black was hand-pressed onto a surface consisting of graphite-beeswax sticky carbon. The well-known anode deactivation due to adsorbed CO, when reformed hydrogen or methanol is used as fuel, has encouraged to extensive research on alternative catalysts, which have better CO tolerance than pure Pt. Pt has been alloyed with different admetals such as Ru and Os [13–15], which provide surface oxygen at lower potentials than Pt does for the oxidative removal of the adsorbed CO. Ir has also been used in the metal alloys. Ir is known to modify the C–H bond in the methanol molecule and thus enables its dehydrogenation [13]. The major potential losses in a PEMFC are due to the sluggish oxygen reduction reaction (ORR) on the cathode. Several hydrodynamic studies on the ORR kinetics can be found. The investigations have been made with different types of electrodes such as Pt/C powders [16] or Pt nanoparticles [17] in Nafion films, Nafion coated Au electrodes [18] or GC electrodes [19] and Pt/C on GC [20]. The Pt particle size effect on the ORR in 0.5 M H_2SO_4 has also been studied [21]. In the study, the optimal size for Pt particles supported on carbon was determined to be 3.5 nm. The structure sensitivity of the ORR was again studied by Perez et al. [22] by a hanging meniscus rotating disc technique.

* Corresponding author. Tel.: +358-2-215-3200; fax: +358-2-215-4962.
E-mail address: ukoponen@abo.fi (U. Koponen).

0378-7753/03/$ – see front matter © 2003 Elsevier Science B.V. All rights reserved.
doi:10.1016/S0378-7753(03)00079-X

In the study they used Pt single crystal electrodes in both H_2SO_4 and $HClO_4$ electrolytes. They found that the (1 1 0) surface was the most active one in both electrolytes followed by the (1 1 1) and (1 0 0) surfaces in H_2SO_4 whereas the order was the opposite in the $HClO_4$ case. Moreover, the effect of the presence of chloride ions on the ORR has also been investigated by using both polycrystalline Pt [23] and Pt single crystal electrodes [23,24]. It has also been reported that the catalytic activity towards the ORR can be improved by alloying Pt with base metals [25] such as Co, Cr, Fe and Ni [26–28]. In the present work, fuel cell catalyst materials have been characterized by cyclic voltammetry. Laboratory made Pt catalyst inks were electrochemically modified with Ru, Os and Ru + Ir. The methanol oxidation activity of the created surfaces was also tested. A novel electrode is introduced which enables the study of the cathode side in such a way that both the oxygen content and the proton activity of the electrolyte can be varied. In situ cyclic voltammetry measurements were also made in a single fuel cell test-fixture to assess active catalyst surface areas in MEAs based on Pt, Pt-Ru and Pt-Co.

2. Experimental

2.1. Preparation of Pt/C and Pt-Co/C electrocatalysts

Catalyst powders were prepared by reducing $PtCl_2$ and $CoCl_2$ metal salts [29]. Hydrotriorganoborates were used in the synthesis to facilitate the formation of nano-sized powders. The metal salt was dissolved in tetrahydrofurane (THF) after which the carbon carrier material (Vulcan XC72, E-TEK) was added to the solution. $LiB(C_2H_5)_3H$ (1 M in THF) was then added slowly to the solution at 60 °C. After a 16–20 h sedimentation, the solution was removed. The powder was consecutively washed with THF, ethanol, THF, and pentane. The prepared Pt/C catalyst powder was characterized by XRD powder diffraction (Philips X'Pert) using a Mo Kα radiation source. The average Pt particle size was determined from line broadening as 4.5–5.5 nm. The Pt content in the powder was 20%. The prepared Pt-Co (1:1) catalyst was characterized for particle morphology and elemental composition using transmission electron microscopy (TEM, Philips CM200 FEG/scanning transmission electron microscopy (STEM)) and scanning transmission electron microscopy coupled with energy dispersive X-ray emission spectroscopy (EDS). The Pt-Co particles were crystalline and according to STEM/EDS elemental point and high magnification (1000k−2000k×) mapping analyses, the majority of the particles were composed of Pt and Co. The particle size was about 2–3 nm and the metal content in the powder was 20%. The laboratory made Pt/C catalyst powder was made into an ink by mixing 500 μl Nafion solution and 4.4 mg of the catalyst powder in an ultrasonic bath for 30 min. A Pt-Co catalyst ink was made as follows: the laboratory made catalyst powder was mixed for 4 h with 5% Nafion solution (in methanol) in an ultrasonic bath. Tetrabutylammonium hydroxide (TBAOH) was then added to the mixture which was stirred continuously for several hours. The ink was then conditioned to proper consistency by adding H_2O and glycerol [30]. For the half-MEA measurements a catalyst layer was prepared by coating a Nafion 117 membrane with Pt ink [31]. The ink was prepared by the method described above but using a commercial Pt/C powder (E-TEK 20% Pt on Vulcan XC-72R, average Pt particle size of 2.5 nm, 112 $m^2\,g^{-1}$ Pt surface area). The membrane was pre-treated by boiling for 1 h in 5% H_2O_2. After rinsing, the membrane was consecutively boiled for 1 h in 0.5 M H_2SO_4, H_2O and 0.5 M NaOH. The membrane was then rinsed and left to stand in water before spreading the catalytic layer. The ink-coated membrane was then dried and heat-treated. Scanning electron microscopy photographs showed that a porous layer consisting of Pt/C particles was formed. Before the experiments, the half-MEA was boiled in 0.5 M H_2SO_4. In single fuel cell catalyst characterization, MEAs consisting of catalyst inks based on Pt/C (E-TEK), Pt-Ru/C (E-TEK) and Pt-Co/C (laboratory made) were used. The MEAs were prepared in the same way as the half-MEAs but spraying ink on both sides of Nafion 115 and 117 membranes.

2.2. Characterization of electrocatalysts

The characterization and modification of the laboratory made Pt ink based on Nafion was carried out with an impinging jet flow cell [32]. Approximately 1 μl of ink was spin-coated onto an Au electrode of 3 mm in diameter and dried under an IR-lamp for 15 min. The typical mass of the ink was 400 μg corresponding to a Pt loading of approximately 1 mg cm^{-2}. The ink was modified by electrodepositing Ru (Aldrich, 10^{-4} M), Os (Acros, 10^{-4} M) and both Ru and Ir (Aldrich, 10^{-4} M) at 0.2 V using various deposition times. The admetal containing solutions were made by dissolving the corresponding metal salt in 0.5 M H_2SO_4 electrolyte (Merck, suprapur, Millipore MilliQ water). The effect of the modification on oxidation of 0.6 M (in 0.5 M H_2SO_4 electrolyte) methanol solution (Baker) was tested at 0.6 V. The containers for both the electrolyte and electrolyte containing admetals were bubbled with Ar (99.998%) before the experiment in order to remove any oxygen. All potentials were determined against a reversible hydrogen electrode. In order to be able to measure and quantify the parameters affecting the active surface area of the catalyst on the cathode side, a novel electrode was designed that enables measuring of the half-MEA (13 mm in diameter) in such a way that the oxygen content on the ink side of the half-MEA can be varied and correspondingly also the proton activity of the electrolyte impinging onto the Nafion side of the half-MEA can be adjusted. The set-up presented in Fig. 1A is made up of a half-MEA that is pressed between a gas-diffuser plate made of Au (fitted inside the electrode housing) and a support ring

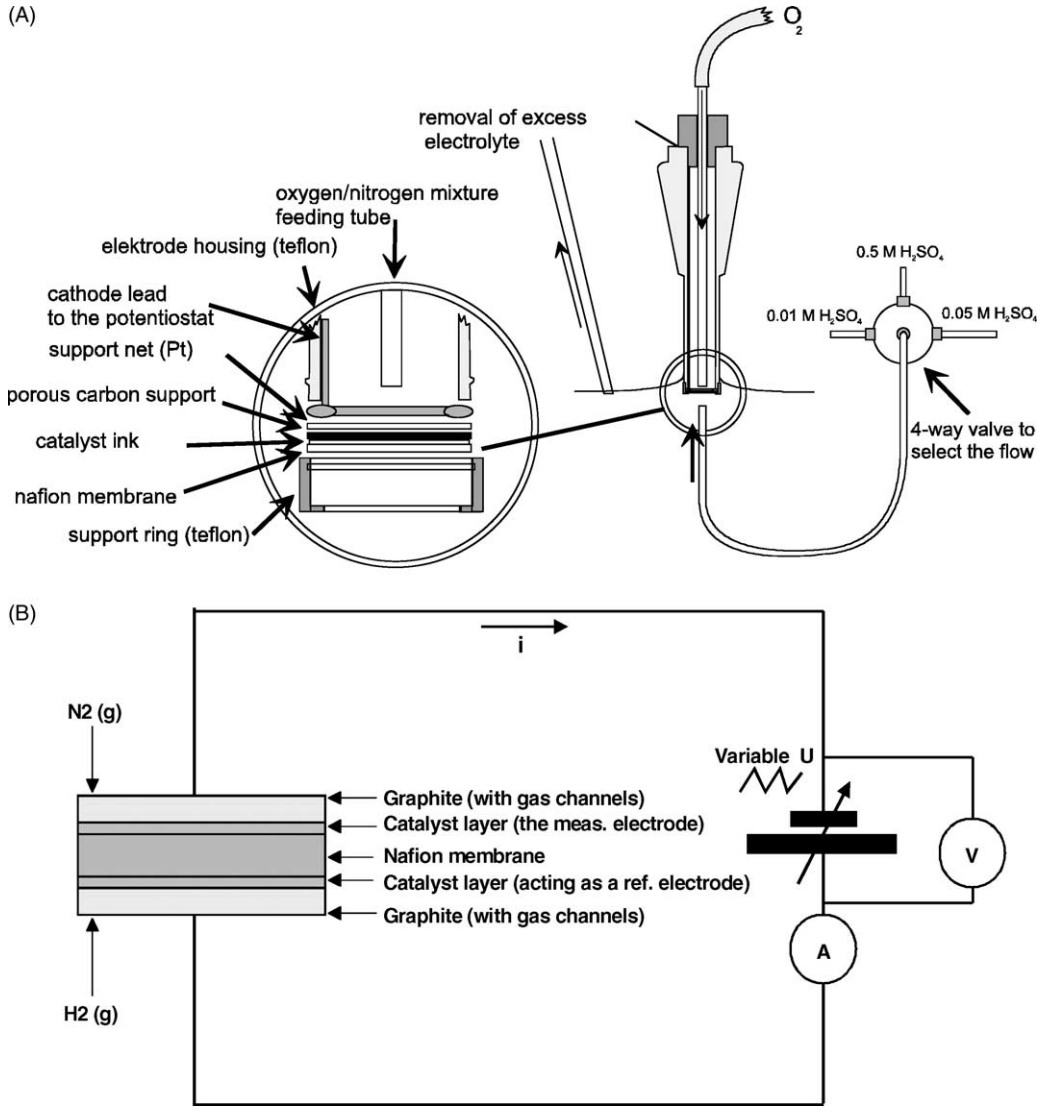

Fig. 1. (A) Schematic presentation of a measuring device for half-MEA investigation. The main components are described in the picture. (B) Set-up of a measuring system for in situ determination of the active catalyst surface area inside a PEM-unit cell.

made out of Teflon. In this way, a connection can be made that prevents the leaking of electrolyte into the back (gas)-side of the half-MEA without the risk of damaging it. As seen from Fig. 1A, the half-MEA is in contact with the gold diffuser plate through porous graphite felt to ensure an even gas distribution. A gold wire is attached to the diffuser plate connecting the MEA with the potentiostat. An O_2/N_2 mixture is fed through the graphite felt into the catalyst structure, and its ratio can be adjusted for instance by adjusting the rotation speeds of the peristaltic gas-feeding pumps. Catalyst layers in a single fuel cell test-fixture were also characterized in situ by cyclic voltammetry. The electrode area in the unit cell was 5 cm^2. The measurements were based on a two-electrode arrangement [33]. Fig. 1B illustrates the schematic of the set-up. One of the electrodes was flushed with H_2 (99.9990%) flow and acted as the reference electrode whereas N_2 (99.99990%) was allowed to flow on the measuring electrode. Prior to the characterization the gases were humidified at atmospheric pressure in gas washing bottles with fine sinters placed in a water bath and piped to the electrodes via gas channels of graphite plates. The current densities are given with respect to the geometric area of the characterized electrodes.

3. Results and discussion

3.1. Continuous oxidation of methanol on modified Pt ink electrodes

The Au electrode spin-coated with laboratory made Pt ink was put into the electrochemical impinging jet flow cell and a hanging meniscus configuration was established. The electrode surface was cleansed by sweeping the potential between 0.05 and 1.35 V at 0.025 V s^{-1} until a stable voltammogram was obtained. The upper potential was

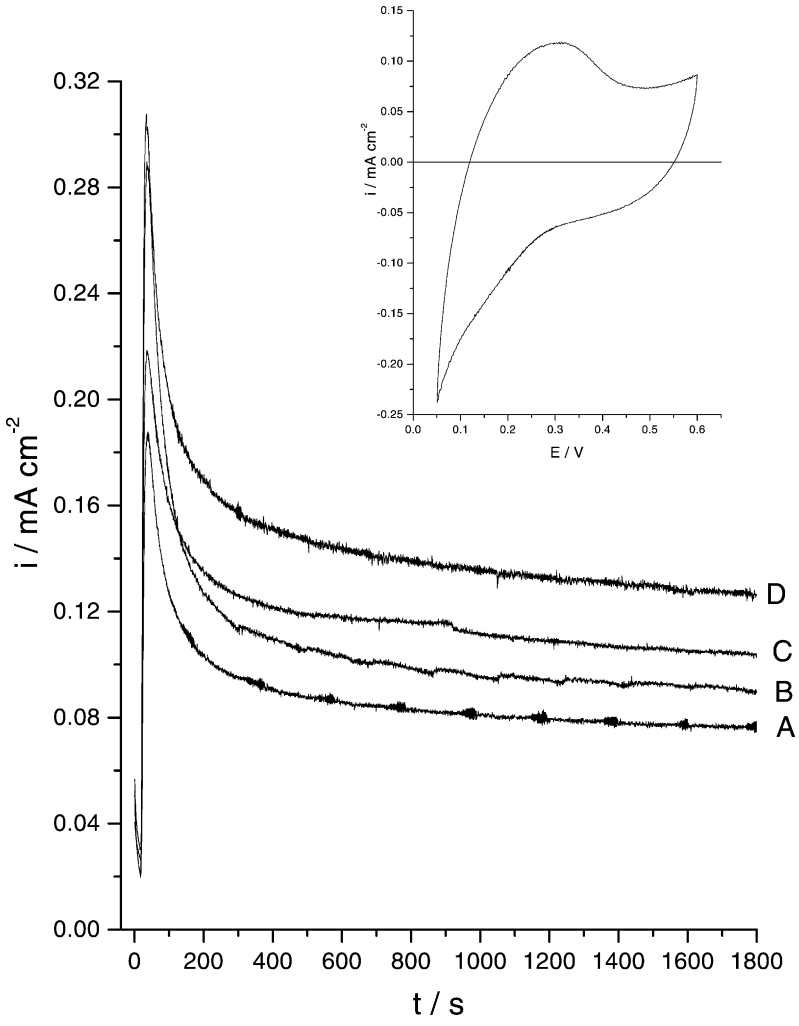

Fig. 2. *Inset*: Voltammogram obtained on Nafion based Pt ink at 0.01 V s^{-1} in 0.5 M H_2SO_4. *Main figure*: Current–time curves at 0.6 V in 0.6 M methanol solution (in 0.5 M H_2SO_4) for laboratory made Pt inks modified with different admetals. (A) pure Pt ink, (B) Pt ink + 90 s Os, (C) Pt ink + 90 s Ru, (D) Pt ink + 90 s Ru + 30 s Ir. The metal adlayers were created by electrodepositing at 0.2 V in 0.5 M H_2SO_4 electrolytes containing 10^{-4} M $RuCl_3$, $OsCl_3$ and $IrCl_3$.

chosen as 1.35 V to avoid getting any contribution from the oxidation of the Au substrate in the recorded voltammograms. The end potential was then changed to 0.6 V and the potential sweeping was continued until a stable Pt voltammogram was obtained. In the inset of Fig. 2, the Pt ink voltammetry is depicted. As seen the hydrogen peaks of the Pt crystallites are not well-defined. One explanation could be that features of the carbon support mask the hydrogen desorption characteristics of Pt [34]. The Pt ink was modified with Ru, Os and consecutively with both Ru and Ir by in situ electroreduction at 0.2 V. By a computer controlled rotating valve it was possible to select the wanted admetal dose, which was then transported by the carrier electrolyte (0.5 M H_2SO_4) to the ink electrode. The effect of the admetal deposition on the ink base voltammetry was not as pronounced as when modifying Pt-bead electrodes with Ru and Os [35,36]. For example, there could hardly be observed any decrease in the hydrogen activity in the potential region between 0.05 and 0.3 V. When long dosing times were used (>30 s), the hydrogen activity even increased. This could probably be explained by the fact that the admetals might deposit onto the carbon or in the Nafion matrix instead of onto the Pt crystallites. The hydrogen activity is thus increased since both Ru and Os are also active towards hydrogen to some extent in this potential interval [36,37]. Despite these deposition characteristics, the admetal modification had a positive effect on the poisoning rate of the Pt surface during methanol oxidation as shown below. Methanol oxidation experiments were carried out on the created catalyst surfaces at 0.6 V in 0.6 M methanol flow for 30 min. After each oxidation experiment the admetal layer was stripped from the surface by 10 potential excursions up to 1.35 V. The electrochemical cell was also rinsed with electrolyte between the experiments. In Fig. 2, the obtained current–time curves are shown for some of the modified Pt ink surfaces. The currents depicted in this figure were obtained on Pt ink surfaces modified with Ru and Os doses of 90 s duration. Ir was dosed for 30 s onto a Ru modified Pt

ink. As a comparison, the current measured using pure Pt ink is also depicted. As seen the modified Pt inks possess higher methanol oxidation rates than the pure Pt ink. The highest activity towards methanol oxidation is obtained with a Pt ink modified with both Ru and Ir. The Os modified ink shows the lowest methanol oxidation activity of the surfaces tested.

3.2. Half-MEA characterization of the ORR on the cathode side

The test electrode introduced in Section 2 was used in the set of experiments described below. A half-MEA consisting of a membrane (Nafion 117) with Pt catalyst ink (0.36 mg Pt cm^{-2}, E-TEK) on its one side, the other one being in its genuine state, was used as the working electrode. The cathode characteristics were investigated by immersing the measuring electrode into the impinging jet flow system and a hanging meniscus configuration was established. The electrode potential was then swept between 0.05 and 0.6 V at 0.01 V s^{-1}. In Fig. 3, curve A shows the stable Pt base voltammetry in 0.5 M H_2SO_4 of the half-MEA. The catalyst surface was cleansed by flushing CO [38] into the ink side of the half-MEA for 3 min (CO flow of 5 ml min^{-1}), after which the electrode was flushed with N_2 for 10 min (N_2 flow of 8 ml min^{-1}). The adsorbed CO was then removed from the surface by a single potential sweep up to 1.1 V. Curve B in Fig. 3 depicts the Pt voltammetry after the cleansing procedure. As seen, the charge in the potential interval between 0.05 and 0.3 V has increased indicating a removal of impurities present in the ink. The electroactive Pt surface area after the CO cleansing was determined to 100 cm^2 mg^{-1} Pt, assuming that 200 μC is consumed per cm^2 surface Pt. The electrolyte concentration was changed to 10 mM by choosing the proper electrolyte flow by the rotating valve. The O_2 flow used on the ink side of the electrode was established to 4 ml min^{-1}. The ORR was carried out chronoamperometrically by increasing the electrode potential in steps of 0.005 V from 0.960 to 1.010 V. At every step the system was allowed enough time to reach its steady state current. In Fig. 4, the Tafel plot for the ORR is shown. A relative straight line was obtained but the slope was determined to be −114 mV dec^{-1}. A Tafel slope of same order of magnitude (−95 mV dec^{-1}) as in the current study was obtained by Srinivasan et al. [34]. In their work they studied the ORR in a PEMFC consisting of electrodes by Prototech (35 mg Pt cm^{-2}) hot-pressed onto Nafion membranes. They suggested that the comparatively steep Tafel slope originated from the combined effects of activation and ohmic control. This is probably also true for the steep slope observed in this study.

3.3. In situ characterization of catalyst layer inside a PEM-unit cell

In situ characterization of catalyst layers inside a PEM-unit cell was carried out with the set-up depicted in Fig. 1B. At elevated temperatures the obtained cyclic voltammograms showed resistive features. This was possibly due to insufficient humidity of the feeding gases. Thus, the voltammograms presented in the following are recorded at room temperature. Prior to the characterization experiment an *I–U* curve for the unit cell was taken where after the cell was let to cool down. The voltammetric characterization was

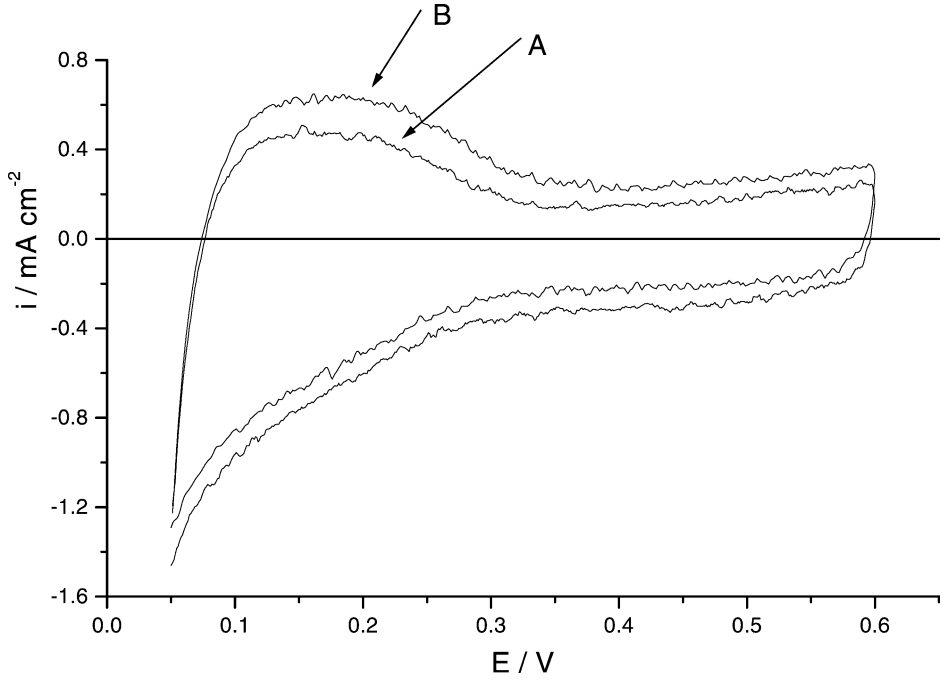

Fig. 3. Pt-based voltammetry for a half-MEA in 0.5 M H_2SO_4 at 10 mV s^{-1}. (A) Before and (B) after CO cleansing. CO was flushed for 3 min through the electrode. Sweep rate: 0.010 V s^{-1}.

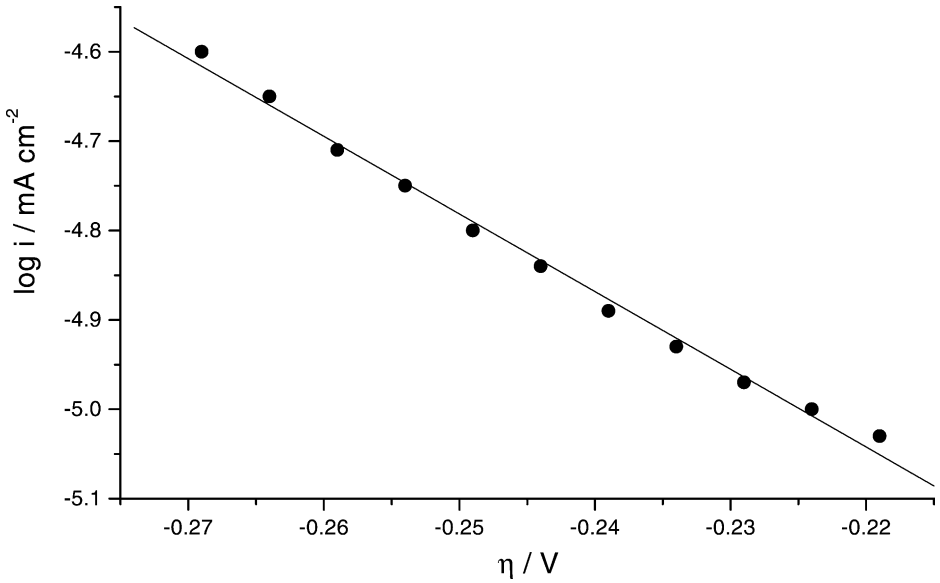

Fig. 4. Tafel plot for oxygen reduction reaction. The test electrode presented in Fig. 1A was used for the determination. Oxygen flow on the ink side: 4 ml min^{-1}. Proton concentration on the membrane side: 10 mM.

made on both sides of the MEA. The catalyst layers were activated and cleansed from any organic impurities by five potential excursions between 0.05 and 1.5 V at 0.3 V s^{-1}. Then the potential was swept between 0.05 and 0.6 V until a stable voltammogram was obtained. Fig. 5 shows examples on voltammograms for catalysts used in the unit cell. In Fig. 5A, the base voltammetry of a Pt the catalyst layer is depicted. The Pt content of the membrane is 0.32 mg cm^{-2}. In the potential interval between 0.1 and 0.3 V, some fine structure of the two hydrogen desorption peaks characteristic for polycrystalline Pt [35,36] can be distinguished. The active Pt surface area was determined to 340 cm^2 mg^{-1} Pt. A membrane consisting of Pt-Ru (E-TEK) was also characterized inside the single fuel cell unit. The metal content in the membrane is 0.42 and 0.21 mg (Pt and Ru) cm^{-2}, respectively. The base voltammetry of the Pt-Ru membrane is seen in Fig. 5B. Here only a single hydrogen desorption peak can be distinguished. The voltammetry resembles that of Pt–Ru alloy electrodes [39,40]. The current in the double layer region is also higher than when only Pt is present in the membrane. This indicates the formation of oxygen containing species such as Ru(II) oxide/hydroxide [41] already at these potentials. In Fig. 5C, the base voltammetry of a MEA consisting of a laboratory made Pt-Co (1:1) catalyst ink is depicted. The metal alloy content is 0.33 mg cm^{-2}. Here a well-defined hydrogen desorption peak between 0.1 and 0.2 V can be noted. The charge between 0.1 and 0.4 V was determined to 16.5 mC. From this charge the active surface area for Pt in the alloy was determined to 100 cm^2 mg^{-1} Pt. A separate set of experiments was also performed where different amounts of Co were electrochemically deposited onto an Au electrode. This was done to verify that Co does not show any hydrogen adsorption in this potential interval, and the results clearly showed that Co gives no contribution to the hydrogen region charge measured from the alloy. The increasing current in the double layer region at ca. 0.5 V is probably due to Co oxide formation. The hydrogen region charge between 0.1 and 0.4 V was determined for four MEAs containing Pt inks (E-TEK). The calculated values are shown in Table 1 where

Table 1
Measured charges and calculated shares of electroactive Pt surface area for MEAs inside a PEM-unit cell

MEA	Mass density of Pt		Measured charge		(C/cm^2)/(mgPt/cm^2)		(Area based on charge)/(geometric area)[a]	
	Side I (mg/cm^2)	Side II (mg/cm^2)	Side I (C/cm^2)	Side II (C/cm^2)	Side I (C/mgPt)	Side II (C/mgPt)	Side I (%)	Side II (%)
1	0.1	0.31	0.008	0.023	0.079	0.074	35	33
2	0.11	0.32	0.007	0.022	0.064	0.070	29	31
3	0.17	0.22	0.014		0.083		37	
4	0.08	0.30	0.005	0.020	0.067	0.066	30	29

The MEAs were prepared by spraying Pt (E-TEK) inks onto Nafion 115.
[a] Share of electroactive Pt.

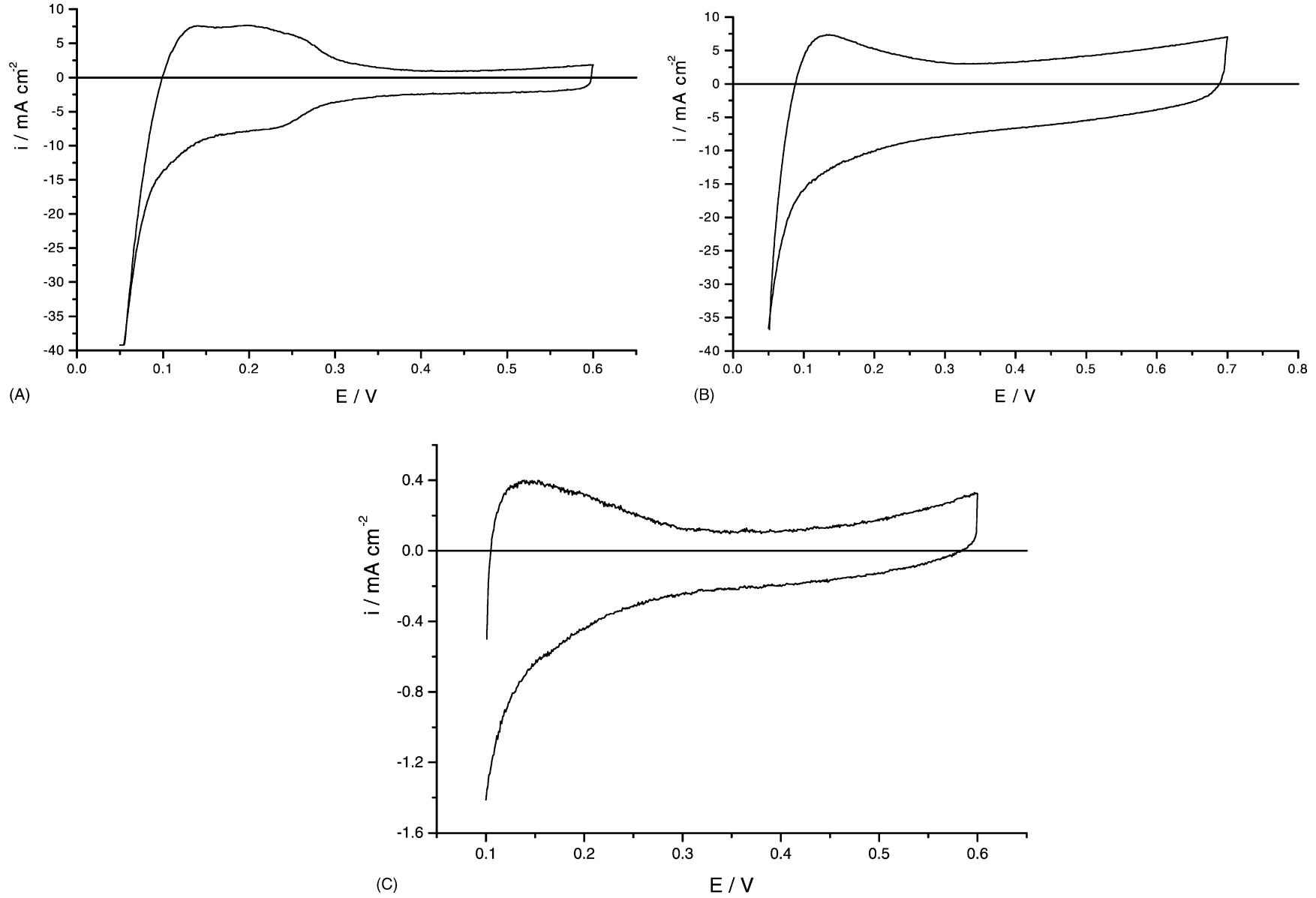

Fig. 5. Cyclic voltammograms on catalyst layers inside a PEM-unit cell. (A) Pt (by E-TEK) catalyst layer on Nafion 115 (0.36 mg Pt cm^{-2}). (B) Pt-Ru (by E-TEK) catalyst layer on Nafion 115 (0.42 and 0.21 mg (Pt and Ru) cm^{-2}, respectively). (C) Laboratory made Pt-Co (1:1) catalyst layer on Nafion 117 (0.33 mg metal alloy cm^{-2}). Electrode area: 5 cm^2. Sweep rate: (A) 0.050 V s^{-1}, (B) and (C) 0.010 mV s^{-1}.

also the Pt mass densities of the MEAs are given. The charges per mass unit Pt were calculated from the measured charges and the mass densities. The last two columns show the shares of electroactive Pt obtained by comparing the voltammetrically determined surface area with the geometric one. The latter of the two areas was obtained from the mass density and the data of the catalyst ink supplier (Pt specific area 112 $m^2\ g^{-1}$). The specific area has been calculated on the basis of the spherical particle assumption and the particle diameter. On this basis it is evident from Table 1 that on the order of 30% of the Pt in the catalyst layers is electroactive. The data in Table 1 also indicates that the active Pt surface areas are linearly dependent on the Pt mass density. In order to determine whether the electroactive surface area of the Pt catalyst inside the PEM-unit cell decreases as a function of time, cyclic voltammograms were recorded during 150 h (totally 26 voltammetric characterizations) for one of the MEAs containing 0.32 mg Pt cm^{-2}. The measurements showed that the Pt surface area did not decrease notably during this time period. During the first 15 h, it decreased about 7% and furthermore approximately 4% during the next 150 h where after it reached a steady state value.

4. Conclusions

Catalyst inks, catalyst layers in both half-MEAs and inside a PEM-unit cell has been characterized by cyclic voltammetry. By means of an impinging jet flow cell it was possible to characterize and modify Pt/C/Nafion inks spin-coated on Au substrate. The effects of the admetal modification on the catalytic activity were further tested by methanol oxidation experiments. The obtained current–time curves showed that the modification had a positive effect on the poisoning rate of the Pt surface. The observations were similar to those obtained using modified Pt-bead electrodes. A Pt ink modified with both Ru and Ir showed the highest oxidation rate among the surfaces tested. The impinging jet flow cell approach was further combined with half-MEA testing. The test electrode presented in this study worked as expected with respect to the effects of the potential and oxygen flow rate at the cathode as well as proton concentration on the membrane solution side. A Tafel slope of -114 mV dec^{-1} was obtained when using 4 ml min^{-1} oxygen flow and 10 mM proton concentration. The steep slope was probably due to the combined effects of activation and ohmic control. In situ voltammograms were useful in assessing the electroactive surface area of catalyst layers inside a PEM-unit cell. It must be noted, however, that in order to obtain comparable results the measurements have to be performed in an identical way, i.e. the membrane history has to be taken into account. Coarsely 30% of the Pt in the catalyst layers proved to be electroactive. The Pt mass density did not significantly affect the electroactive surface area per mass unit catalyst.

Acknowledgements

This work was financially supported by the National Technology Agency of Finland (Tekes). The support of the Graduate School of Materials Research is gratefully acknowledged. Useful advice by Tuomas Mennola, Helsinki University of Technology, is also acknowledged.

References

[1] T.J. Schmidt, H.A. Gasteiger, R.J. Behm, P.M. Urban, D.M. Kolb, J. Electrochem. Soc. 145 (1998) 2354.
[2] H. Wang, C. Wingender, H. Baltruschat, M. Lopez, M.T. Reetz, J. Electroanal. Chem. 509 (2001) 163.
[3] J. Shan, P.G. Pickup, Electrochim. Acta 46 (2000) 119.
[4] Y. Takasu, T. Iwazaki, W. Sugimoto, Y. Murakami, Electrochem. Commun. 2 (2000) 671.
[5] Y. Takasu, Y. Fujii, K. Yasuda, Y. Iwanaga, Y. Matsuda, Electrochim. Acta 34 (1989) 453.
[6] K. Yahikozawa, Y. Fujii, Y. Matsuda, K. Nishimura, Y. Takasu, Electrochim. Acta 36 (1991) 973.
[7] S. Park, A. Wasileski, M.J. Weaver, J. Phys. Chem. B 105 (2001) 9719.
[8] K.A. Friedrich, F. Henglein, U. Stimming, W. Unkauf, Electrochim. Acta 45 (2000) 3283.
[9] S.N. Pron'kin, G.A. Tsirlina, O.A. Petrii, S.Yu. Vassiliev, Electrochim. Acta 46 (2001) 2343.
[10] G. Méli, J.-M. Léger, C. Lamy, J. Appl. Electrochem. 23 (1993) 197.
[11] E.R. Savinova, N.P. Lebedeva, P.A. Simonov, G.N. Kryukova, Russ. J. Electrochem. 36 (2000) 952.
[12] J.W. Long, K.E. Ayers, D.R. Rolison, J. Electroanal. Chem. 522 (2002) 58.
[13] B. Gurau, R. Viswanathan, R. Liu, T.J. Lafrenz, K.L. Ley, E.S. Smotkin, E. Reddington, A. Sapienza, B.C. Chan, T.E. Mallouk, S. Sarangapani, J. Phys. Chem. 102 (1998) 9997.
[14] K.L. Lay, R. Liu, C. Pu, Q. Fan, N. Leyarovska, C. Segre, E.S. Smotkin, J. Chem. Soc. 144 (1997) 1543.
[15] H.A. Gasteiger, N.M. Markovic, P.N. Ross Jr., E.J. Cairns, J. Phys. Chem. 97 (1993) 12010.
[16] F. Gloaugen, P. Convert, S. Gamburzev, O.A. Velev, S. Srinivasan, Electrochim. Acta 43 (1998) 3767.
[17] O. Antoine, Y. Bultel, R. Durand, J. Electroanal. Chem. 499 (2001) 85.
[18] J. Maruyama, M. Inaba, Z. Ogumi, J. Electroanal. Chem. 458 (1998) 175.
[19] J. Maruyama, I. Abe, J. Electroanal. Chem. 527 (2002) 65.
[20] U.A. Paulus, T.J. Schmidt, H.A. Gasteiger, R.J. Behm, J. Electroanal. Chem. 495 (2001) 134.
[21] M. Peuckert, T. Yoneda, R.A. Dalla Betta, M. Boudart, J. Electrochem. Soc. 133 (1986) 944.
[22] J. Perez, H.M. Villullas, E.R. Gonzalez, J. Electroanal. Chem. 435 (1997) 179.
[23] T.J. Schmidt, U.A. Paulus, H.A. Gasteiger, R.J. Behm, J. Electroanal. Chem. 508 (2001) 41.
[24] V. Stamenkovic, N.M. Markovic, P.N. Ross Jr., J. Electroanal. Chem. 500 (2001) 44.
[25] T. Ralph, M. Hogarth, Platinum Metals Rev. 46 (2002) 3.
[26] A.K. Shukla, M. Neergat, P. Bera, V. Jayaram, M.S. Hegde, J. Electroanal. Chem. 504 (2001) 111.
[27] M.-k. Min, J. Cho, K. Cho, H. Kim, Electrochim. Acta 45 (2000) 4211.
[28] T. Toda, H. Igarashi, M. Watanabe, J. Electroanal. Chem. 460 (1999) 258.

[29] H. Bönnemann, W. Brijoux, R. Brinkmann, R. Fretzen, T. Joussen, R. Köppler, B. Korall, P. Neiteler, J. Richter, J. Mol. Catal. 86 (1994) 129.
[30] M.S. Wilson, S.J. Gottesfeld, J. Electrochem. Soc. 139 (1992) L28.
[31] M.S. Wilson, US Patent 5,211,984 (1993).
[32] M. Berelin, M. Wasberg, J. Electroanal. Chem. 449 (1998) 181.
[33] X. Cheng, B.Y. Yi, M. Han, J. Zhang, Y. Qiao, J. Yu, J. Power Sources 79 (1999) 75.
[34] S. Srinivasan, E.A. Ticianelli, C.R. Derouin, A. Redondo, J. Power Sources 22 (1988) 359.
[35] S. Szabo, I. Bakos, J. Electroanal. Chem. 230 (1987) 233.
[36] U. Koponen, M. Bergelin, M. Waseberg, J. Electroanal. Chem. 531 (2002) 87.
[37] S. Szabó, I. Bakos, F. Nagy, J. Electroanal. Chem. 271 (1989) 269.
[38] U. Koponen, T. Peltonen, M. Bergelin, T. Mennola, M. Valkiainen, J. Kaskimies, M. Wasberg, J. Power Sources 86 (2000) 261.
[39] D. Chu, S. Gilman, J. Electrochem. Soc. 143 (1996) 1685.
[40] H. Hoster, T. Iwasita, H. Baumgärtner, W. Vielstich, J. Electrochem. Soc. 148 (2001) A496.
[41] T. Frelink, W. Visscher, J.A.R. van Veen, Langmuir 12 (1996) 3702.